

1 Stiffness evolution of natural hydraulic lime mortars at early ages 2 measured through EMM-ARM

3 Lucía Garijo^a, Miguel Azenha^{b,1}, Meera Ramesh^b, Paulo B. Lourenço^b, Gonzalo Ruiz^a

4 ^a*ETS de Ingenieros de Caminos, C. y P., Universidad de Castilla-La Mancha. Avda. Camilo José Cela,*
5 *s/n, 13071 Ciudad Real, Spain*

6 ^b*ISISE – Instituto para a Sustentabilidades e Inovação em Estruturas de Engenharia, Universidade do*
7 *Minho, Escola de Engenharia, Campus de Azurém, 4800 Guimarães, Portugal*

9 **ABSTRACT:**

10 This paper focuses on the mechanical characterization of the early age behavior of three NHL mortars
11 with different water/lime ratios. A vibration-based technique with continuous data recording (Elastic
12 Modulus Measurement through Ambient Response Method - EMM-ARM) was used to measure stiffness
13 of the different mortars that were found to range between 2.5 and 4.1 GPa on day 7. Other physical and
14 mechanical properties such as strength and density were measured as a function of sample preparation
15 protocols –vibrated, compacted, sealed and unsealed. After 7 days, sealed specimens led to 50% lower
16 compressive strength and 25% lower flexural strength compared to unsealed specimens.

17
18 **KEYWORDS:** Natural Hydraulic Lime (NHL) mortars, Elastic Modulus Measurement through
19 Ambient Response Method (EMM-ARM), Stiffness evolution, Ultrasonic pulse velocity test (UPV),
20 Sample preparation.

21 **1. INTRODUCTION**

22 Natural hydraulic lime mortars, henceforward referred to as NHL, are widely used for restoration of
23 historic buildings and structures (particularly in the case of masonry) due to their good compatibility with
24 the substrate material and eco-efficiency (hydraulic lime consumes low amount of energy during its

¹Corresponding author.

Email address: miguel.azenha@civil.uminho.pt (M. Azenha).

25 production process in comparison with cementitious materials, and it naturally absorbs environmental
26 carbon dioxide after being applied in construction) [1]. From the mechanical point of view, NHL mortars
27 are also very suitable for restoration works because they are able to accommodate minor differential
28 movement of masonry over time without cracking [2]. However, despite awareness of the importance of
29 the early age conditions of application, curing and stiffness build-up in the actual behavior of NHL
30 mortars, little research is found about the behavior of these mortars at early ages. For instance, Lanas
31 *et al.* [3] performed flexural and compression tests and thermogravimetric analyses (TGA) on mortars
32 with NHL type 5 at 3 and 7 days. Arandigoyen and Alvarez [4] tested aerial lime mortars with cement in
33 bending and compression after 3 and 7 days. However, the literature review conducted in the scope of this
34 paper did not encounter any study/report focused on the stiffness evolution of NHL mortars at early ages,
35 particularly including the first 48h of hardening. This is of crucial importance because the behavior of
36 NHL mortars at early ages has a direct influence on the supporting capability and ability to accommodate
37 movements of masonry during construction or repairing operations. This behavior is especially relevant
38 for interventions in historic structures, where an appropriate large deformation before failure of the new
39 additions helps to avoid brittle breakage when restrained by preexistent elements.

40 For these reasons, the objective of this research is to study the behavior of three NHL mortars at early
41 ages (same binder, with three distinct water/binder ratios). An exhaustive mechanical and physical
42 characterization of these mortars was performed, including the measurement of the elastic modulus
43 through two methods: *Elastic Modulus Measurement through Ambient Response Method* (EMM-ARM)
44 [5], and *Cyclic Compression* test (CC) on cylinders. Furthermore, the following tests and property
45 assessments have also been deployed: penetration resistance test to study the initial setting time of the
46 mortars; density and normalized flexural and compressive strength tests on prisms at days 2, 4 and 7;
47 open porosity and, finally, thermogravimetric analysis on the corresponding lime paste to study the
48 evolution of portlandite ($\text{Ca}(\text{OH})_2$) content that results from the hydration of the NHL compounds,
49 (mainly C_2S) [3].

50 One of the most striking novelties of this research lies on the pioneering application of the
51 EMM-ARM technique to NHL mortars. This test allows automatic and continuous evaluation of the
52 Elastic Modulus immediately after casting without demolding the specimen. EMM-ARM is based on the
53 continuous evaluation of the resonance frequency of the tested specimen (simply supported composite

54 beam), which can in turn allow direct evaluation of the tested material through application of the dynamic
55 equation of motion of the system [5-9]. For further comprehension of the early age behavior of NHL
56 mortars, some relations were established among the results of the several conducted tests. In such way,
57 EMM-ARM was compared with the results of CC on one reference mortar and penetration resistance
58 tests on the three NHL mortars. Due to the nature of the EMM-ARM testing adopted, as well as its
59 principles of operation, the test specimen is relatively slender (50.5 cm long cylinder), and the specimen
60 needs to be kept within the mold during testing, in order to keep the same mechanical boundary
61 conditions and avoid mass losses. These experimental requirements of EMM-ARM led to the need for
62 vibration in the preparation of EMM-ARM samples (due to the long and thin mold), and the specimens
63 were constantly sealed. These vibrated/sealed conditions do not match the fabrication/curing conditions
64 required in the standards for NHL [10], which include compaction with 25 strokes of the tamper and
65 unsealed curing conditions. Also, keeping the specimens sealed hinders the process of carbonation, which
66 plays a role in the hardening of NHL mortars as well. For that reason, EMM-ARM, as performed herein,
67 was limited to the maximum age of 7 days, during which the effects of carbonation would presumably
68 still have been minor as in the case of unsealed curing. Anyhow, it was important to ascertain the impact
69 of fabrication (compaction/vibration) and curing (sealed/unsealed) conditions in the studied NHL mortars
70 so as to allow further conclusions to be drawn from the obtained results. Density, flexural and
71 compressive strength tests were carried out on samples with different preparation and curing methods: the
72 standard one (compacted with 25 strokes of the tamper and unsealed), the one followed in the preparation
73 of EMM-ARM specimens (vibrated and sealed) and an additional one (compacted and sealed). In such
74 way, it was possible to relate the results of such tests implying stiffness and strength measurements.
75 Furthermore, some relations were also established among the results of density, ultrasonic pulse velocity
76 (UPV) and open porosity of the three mortars to better understand the interplay of these properties on the
77 behavior of NHL mortars at early ages. Finally, the evolution of free portlandite content of one reference
78 NHL paste was related to the compressive strength of the corresponding mortar through the performance
79 of thermogravimetric analysis.

80 The rest of the paper is organized as follows. After this introduction, Section 2 describes the materials
81 and experimental procedure, whereas Section 3 pertains to the discussion of attained results, with
82 conclusions being drawn in Section 4.

83 **2. EXPERIMENTAL PROGRAM**

84 **2.1 Raw materials**

85 The three mortars were prepared with a commercial natural hydraulic lime of class NHL 3.5,
86 according to EN 459-1 [11] that was supplied by “Socli, Italcementi Group” (France). It had a density of
87 2.58 g/cm³ and an apparent density of 0.85 g/cm³. Chemical and mineralogical analyses of the natural
88 hydraulic lime, NHL 3.5, are provided in Table 1 and Fig. 1. They were performed by X-ray fluorescence
89 (XRF) and X-ray diffraction (XRD) analyses by using a Philips (PANALYTICAL) Magis Pro X-ray
90 fluorescence spectrometer, and a Philips (PANALYTICAL) X’Pert MPD diffractometer, respectively.

91

92

Table 1. Chemical and mineralogical compositions of the NHL 3.5.

Chemical composition (%)	
Na ₂ O	0.125
MgO	3.078
Al ₂ O ₃	2.051
SiO ₂	13.606
P ₂ O ₅	0.044
SO ₃	0.990
K ₂ O	0.456
CaO	59.949
TiO ₂	0.132
MnO	0.014
Fe ₂ O ₃	0.994
NiO	0.014
CuO	0.007
ZnO	0.004
SeO ₂	0.002
Rb ₂ O	0.003
SrO	0.169
CO ₂	18.365
Mineral phases (%)	
Portlandite, Ca(OH) ₂	40-45
Calcite, CaCO ₃	40-45
Calcium silicates	10-15

93

94

95

96

97

98
 99
 100
 101
 102
 103
 104
 105
 106
 107
 108
 109
 110
 111
 112
 113
 114
 115
 116
 117
 118
 119
 120
 121
 122
 123
 124
 125
 126
 127
 128
 129
 130

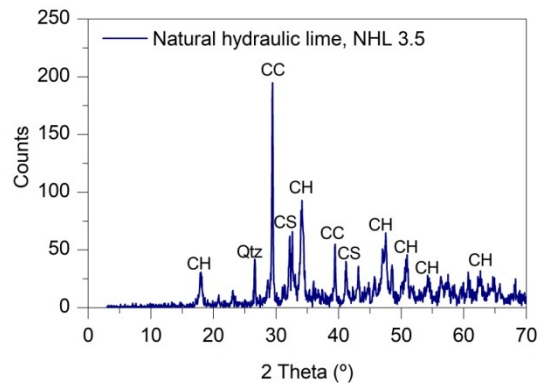


Figure 1: X-ray diffraction pattern of the NHL 3.5. CH = portlandite, CC = calcite, CS = calcium silicates, Qtz = quartz.

Also, the laser particle size distribution curve of the NHL 3.5 was obtained by means of a PSD Mastersizer 3000 from Malvern Instruments, see Fig. 2.

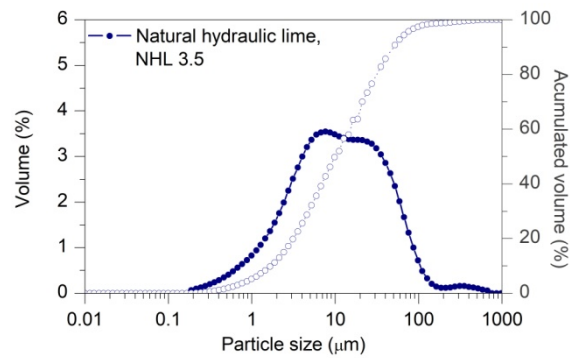


Figure 2: Results of laser particle size distribution for NHL 3.5.

The sand used was commercial crushed limestone of maximum grain size of 4 mm and had a particle size distribution curve- presented in Figure 3, determined according to EN 1015-1 [12]. It had an apparent particle density of 2.68 g/cm³ according to EN 1097-6 [13] and an apparent density of 1.82 g/cm³ according to EN 1097-3 [14].

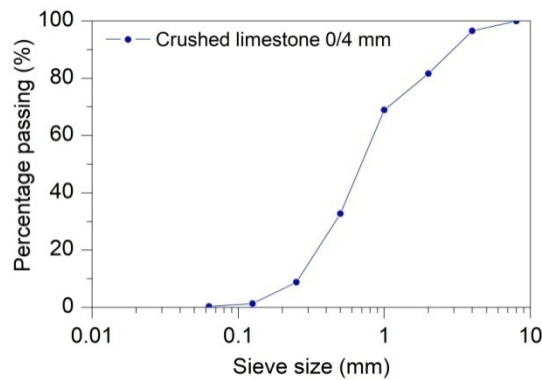


Figure 3: Particle size distribution curve of the aggregate used.

131 **2.2 Mortar composition and preparation**

132 Three mortar compositions were prepared with different water/lime ratios: 0.8, 0.9 and 1.1 by volume,
 133 with the mortars being named as M0.8, M0.9 and M1.1, respectively. The lime/aggregate ratio used for
 134 the three mortars was 1:3 by volume. Volume proportions of compounds were converted into weight so
 135 as to minimize effects of measurement imprecision in the mixing process (see Table 2). Depending on the
 136 water/lime ratio used, three values of consistency were obtained: 130 mm (M0.8 - dry), 155 mm (M0.9 -
 137 plastic) and 240 mm (M1.1 - fluid), determined by the flow table test according to the standards
 138 EN 1015-3 [15] and EN 1015-6 [16]. Considering that plastic consistency is most widely used, mortar
 139 M0.9 (in each of the three different compaction/sealing conditions, S, V and C) has been regarded as the
 140 reference for all tests conducted and properties evaluated in this research work. The mixing process was
 141 performed according to EN 1015-2 [17] by following the procedure for small bowl mixers (in this case
 142 with a capacity of 5 dm³). Different batches of the same mix were cast and repeatability was then checked
 143 for each test.

144 Table 2: Mortar compositions for each NHL mortar

Mortar	Lime/aggregate ratio by volume	NHL (g)	Aggregate (g)	Water (cm ³)	Water/lime ratio by volume	Water/lime ratio by weight
M0.8	1:3	525.2	3367.3	494.3	0.8	0.94
M0.9	1:3	514.5	3298.6	544.7	0.9	1.06
M1.1	1:3	494.3	3169.2	639.7	1.1	1.29

145
 146 Different sizes of specimens, compacting methods and curing conditions were used depending on the
 147 test to be applied (Table 3).The reason for the distinct fabrication conditions employed has been given in
 148 the introduction of this paper. Standard mortars were compacted with 25 strokes of the tamper and cured
 149 unsealed inside a climatic chamber at relative humidity (RH) 95% and 20°C. This humidity is
 150 recommended by EN 1015-11 [10] and is reported to favor the hydration of NHL mortars [18-20]). These
 151 mortars were tested to measure UPV, flexural and compressive strengths and open porosity. In the table,
 152 the column “Type of mortar” includes the nomenclature M0.8, M0.9 and M1.1, with an additional suffix
 153 that clarifies the fabrication/curing conditions: suffix “S” for the standard situation that has just been
 154 described namely – compacted and unsealed (air cured); suffix “V” for vibrated (with a vibration table)
 155 and sealed (inside the PVC tubes of the EMM-ARM samples or covered with two plastic bags in the case

156 of the rest of the samples); suffix “C” for compacted (with 25 strokes of the tamper) and sealed
 157 (following the same aforementioned procedure). All the mortars remained in climatic chambers with
 158 corresponding curing conditions as indicated in Table 3. The days at which the different specimens were
 159 removed from their corresponding molds are also referred to in Table 3. Furthermore, a lime paste
 160 specimen has been prepared for TGA testing, with water to lime ratio of 0.9: P0.9.

161 Table 3: Sizes of specimens, compacting methods and curing conditions of the NHL mortars.

Tests	Specimen shape and dimensions (mm)	Type of mortar	Curing conditions	Compacting method and sealing conditions	Time of demolding
EMM-ARM	Cylinder ϕ 44×505	M0.8V, M0.9V, M1.1V	20°C - sealed	(V) Vibrated and sealed	No demolding
CC	Cylinder ϕ75×150	M0.9S	20°C – RH 95%	(S) Standard	At day 2
CC	Cylinder ϕ75×150	M0.9V	20°C – RH 95%	(V) Vibrated and sealed	Before testing
UPV (discrete measurements) – flexural and compression	Prisms 40×40×160	M0.8S, M0.9S, M1.1S	20°C – RH 95%	(S) Standard	At day 2
UPV (discrete measurements) – flexural and compression	Prisms 40×40×160	M0.8V, M0.9V, M1.1V	20°C – RH 95%	(V) Vibrated and sealed	At day 2
Flexural and compression	Prisms 40×40×160	M0.8C, M0.9C, M1.1C	20°C – RH 95%	(C) Compacted and sealed	At day 2
Open porosity	Prisms 40×40×160	M0.8S, M0.9S, M1.1S	20°C – RH 95%	(S) Standard	At day 2
Open porosity	Prisms 40×40×160	M0.8V, M0.9V, M1.1V	20°C – RH 95%	(V) Vibrated and sealed	At day 2
TGA	N/A (sample of less than 20 mg)	P0.9	20°C – RH 95%	Sealed	Before testing

162

163 2.3 Test procedures

164 2.3.1 Elastic Modulus Measurement through Ambient Response Method (EMM-ARM)

165 The EMM-ARM is a methodology proposed by Azenha *et al.* [5] for cement-based materials. It has
 166 been widely validated for cement pastes [7, 21-23], cement mortars [7], concrete [5, 24] and recently for
 167 aerial lime-cement mortars [25]. In this paper, it was applied for the first time to the study of NHL
 168 mortars. This method allows the automatic and continuous evaluation of the elastic modulus immediately
 169 after casting and it has two fundamental differences compared to conventional resonant frequency
 170 methods (e.g. impact-resonance methods): (i) the resonant frequencies are much lower, well below 1kHz

171 (thus more similar to quasi-static testing); (ii) the specimen is not demolded during testing [23]. The
172 methodology is based on continuous modal identification of the first flexural resonant frequency of a
173 composite beam that is placed horizontally, simply supported at both ends in the case of concrete and
174 some mortars (in contrast with the cantilever beam configuration used for pastes). A typical setup adopted
175 during the present experimental program is shown in Fig. 4. At mid-span of the beam, vertical
176 accelerations resulting from forced vibration with a non-contact magnetic actuator are measured. With
177 this, it is possible to perform modal identification and evaluate the first flexural resonance frequency of
178 the beam. This resonant frequency of the beam is related to the increasing elastic modulus of the tested
179 material by applying the dynamic equation of motion of the system (all variables known except for elastic
180 modulus, which can be directly computed). In this way it is possible to obtain a real-time curve of elastic
181 modulus against time [26].

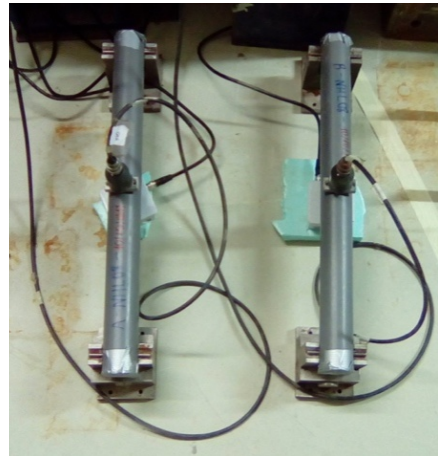


Figure 4: EMM-ARM setup.

182
183
184

185 The specimens used in this study were prepared with a PVC tube with inner/outer diameter of
186 44 mm/50 mm, 550 mm length and with a span of 500 mm between supports. Two specimens per mortar
187 mix were cast and tested (Fig. 4). The mortar was always vibrated as it was introduced in the tubes. After
188 casting, the acceleration measurements could start within a period of less than 30 minutes since the
189 mixing of lime and water. The samples remained sealed in the mold during the whole test for seven days.

190 2.3.2 Cyclic Compression tests (CC)

191 Cyclic Compression (CC) tests were made on cylindrical specimens to measure the elastic modulus at
192 ages of 2, 4 and 7 days on the reference mortars, M0.9S and M0.9V, and compared with the results

193 obtained with EMM-ARM. The specimens had a diameter/height of 75 mm/150 mm. A hydraulic
194 actuator with 25 kN capacity was used for load application, and three Linear Variable Differential
195 Transducers (LVDTs), supported by 2 centered steel rings were attached to the specimens at 120°
196 intervals, with a reference measuring span of 50 mm [23]. The test protocol was similar to the one
197 followed in references [18, 27]: each test involved 5 loading/unloading cycles up to 30% of the maximum
198 load obtained in a compression test performed on one extra cylinder (at the same age of testing). The
199 displacement rate of the cycle to obtain the elastic modulus was 0.7 mm/min (in displacement control to
200 better perform the test at such early ages). After each test, the specimens were broken in compression at
201 10 N/s to evaluate the compressive strength.

202 2.3.3 Penetration resistance tests

203 Penetration tests were applied on the three mortar compositions, M0.8V, M0.9V and M1.1V,
204 according to standard ASTM C-403 [28] for concrete as a reference. A penetrometer by Controls, model
205 54-C0145, was used. The purpose of this test was to obtain the initial setting time of the mixes and
206 compare it with the early singularities of continuous monitoring provided by EMM-ARM. Cubic molds
207 of 150 mm edge length were used. The time of initial setting is measured as the moment when the
208 penetration resistance, measured by the shank of a needle, equals 3.5 MPa.

209 2.3.4 Ultrasound Pulse Velocity tests (UPV)

210 The UPV test is a method that consists in generating a pulse on one side of the sample, which is
211 transmitted through the material and received on the opposite side of the sample. The time delay between
212 the generated and received signals is recorded to obtain the wave travel time through the material. The
213 velocity of the compressional (P) wave, V_p , can be related to the elastic properties of the medium (the
214 dynamic Poisson's ratio, ν_{dyn} , and the dynamic elastic modulus, E_{dyn}) and the density, ρ , through the
215 following equation, which is applicable for homogeneous and isotropic media [23, 29].

$$216 \quad V_p = \sqrt{\frac{(1-\nu_{dyn})E_{dyn}}{(1+\nu_{dyn})(1-2\nu_{dyn})\rho}} \quad (1)$$

217 UPV was measured in some specimens at discrete times in the transverse direction (Fig. 5),
218 particularly in the specimens used for flexural and compressive strength tests. UPV velocity was
219 measured just before the actual mechanical tests. The ultrasound probes had 25 mm diameter and

220 operating frequency of 150 kHz. Probe of this diameter was considered adequate, as it was larger than the
221 largest expected heterogeneity of the mortar. Spacing between the probes was set as 40 mm, longer than
222 two wavelengths at the selected operating frequency [23].

223



224

225 Figure 5: UPV set-up. Discrete measurement in the lateral direction.

226

227 2.3.5 Flexural and compressive strength tests

228 Flexural and compressive strengths were measured at 2, 4 and 7 days. The standard EN 1015-11 [10]
229 was observed. Flexural strength was measured by three-point bending on three 40 mm × 40 mm ×
230 160 mm specimens applying a displacement rate of 0.2 mm/min. Compressive strength tests that were
231 conducted on six of the resulting half-prisms from the flexural strength tests, also employed displacement
232 control at 0.7 mm/min. These were the same displacement rates as the ones adopted in [19], instead of the
233 ones set by the standard, to better control the tests at such early ages.

234 2.3.6 Open porosity

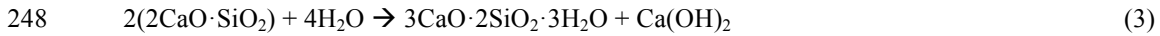
235 Open porosity was measured on the three mortar mixes, particularly M0.8S, M0.9S and M1.1S and
236 M0.8V, M0.9V and M1.1V, at day 7, according to UNE 83980 [30] for concrete as a reference, which is
237 determined according to water saturation. In this test, dry weight of the samples (m_1), weight after water
238 saturation in a vacuum pump (m_3) and apparent weight (m_4) with a hydrostatic balance were measured.
239 The open porosity, OP , in percentage, was then obtained by equation 2.

$$240 \quad OP = \frac{m_3 - m_1}{m_3 - m_4} 100 \quad (2)$$

241 2.3.7 Thermogravimetric analyses (TGA)

242 In thermogravimetric analysis (TGA), a material sample is submitted to a defined rate of temperature
243 change until a maximum value is reached [31-33]. The mass of the sample is monitored through the
244 temperature range, and a resulting graph can be plotted with weight vs. temperature – TGA curve [31-34].

245 In this study, thermogravimetric analyses were performed on the lime paste of the corresponding
246 reference mortar, P0.9 at day 0, 2, 4 and 7 to study the evolution of hydration by means of free
247 portlandite, Ca(OH)_2 , content (Eq. (3)).



249 For this purpose, samples remained sealed until the moment of testing. Before testing, the technique
250 of hydration stoppage with isopropanol according to [35] was applied. Then a sample of less than 20 mg
251 was placed in an aluminum crucible. During the test, a heating rate of 10 °C/min from ambient
252 temperature up to 1000°C was applied so as to allow direct measurement of hydroxide and carbonate
253 compounds at hydroxylation and decarboxylation ranges, respectively [33, 36]. According to [33, 37],
254 dehydroxylation, which is the process of decomposition of calcium hydroxide (Ca(OH)_2), typically occurs
255 in the range 300-550°C, meanwhile the decomposition of calcium carbonate (CaCO_3), termed as
256 decarboxylation, occurs in the range 650-950°C.

257 Once the test is finished, the quantity of calcium hydroxide that is decomposed can be obtained
258 through Eq.(4-5) [35]:

$$259 \quad M_{P,m} = \text{WL}_P \frac{m_P}{m_w} \quad (4)$$

$$260 \quad \text{Per 100g paste: } M_{P,n} = \frac{M_{P,m}}{W_{600}(1+w/b)} \quad (5)$$

261
262 where $M_{P,m}$ is the free portlandite measured, WL_P is the weight loss of the portlandite in the sample, m_P
263 and m_w are the molecular masses of portlandite ($m_P = 74 \text{ g/mol}$) and water ($m_w = 18 \text{ g/mol}$),
264 respectively, $M_{P,n}$ is the normalized free portlandite measured in the paste, W_{600} is the weight of the
265 sample at 600°C and w/b the water/lime ratio.

266 3. EXPERIMENTAL RESULTS AND ANALYSIS

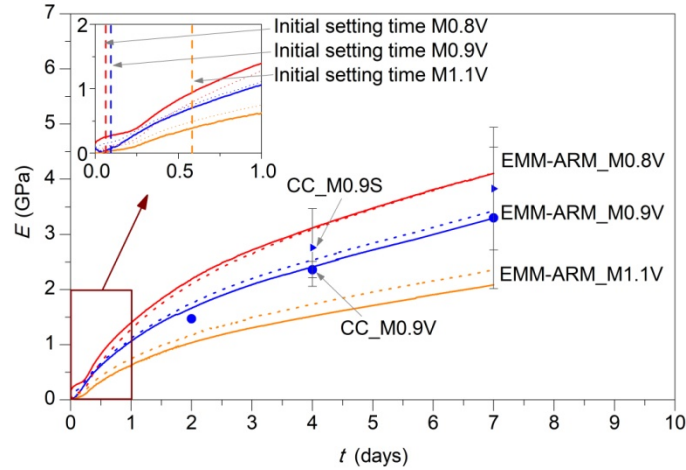
267 3.1 Comparison between monitoring methods

268 First of all, the results of EMM-ARM are shown for the three mortars, M0.8V, M0.9V and M1.1V
269 (Fig. 6). For the reference mortar, M0.9, they were compared to the ones obtained through CC. Results
270 from all three mortars were compared with the initial setting time measured through penetration
271 resistance test.

272 3.1.1 EMM-ARM

273 EMM-ARM curves obtained for the three mortars tested, M0.8V, M0.9V and M1.1V, and comparison
274 with CC for the reference mortars, M0.9V and M0.9S, are shown in Fig. 6. It is worth mentioning that a
275 wide range of elastic modulus was obtained throughout the curing process of the NHL mortars, ranging
276 from 0 GPa to ~4 GPa within the testing period. Furthermore, all elastic modulus evolution curves seem
277 to be plausible, showing a short initial dormant period (with elastic modulus close to 0 GPa), after which
278 elastic modulus evolved significantly for all tested mortars. Then, after around one day, the slope of
279 elastic modulus evolution curves decreased with time within the testing period. From the zoom of graph
280 in Fig. 6, it can be seen that mortar M0.8V (specimen 1) presented some initial stiffness in the early
281 curing hours in comparison to mortars M0.9V and M1.1V. Such initial stiffness is likely to be due to the
282 low viscosity of the mortar stemming from its low water/lime ratio and low value of consistency
283 (120 mm). Mortars M0.9V and M1.1V, with higher water/lime ratios, did not present such initial stiffness
284 as they were more fluid.

285 Two samples per mortar mix were tested as shown in Fig. 6. It is possible to verify the good
286 coherence of the two curves obtained for each mortar, demonstrating adequate repeatability of EMM-
287 ARM. Mortar M0.8V presented especially good repeatability as its elastic modulus curves differed less
288 than 0.17% at day 7. Furthermore, it is also possible to observe that the reduction of the water/lime ratio
289 increases early hydration rates and leads to higher values of elastic modulus. For example, at day 7, the
290 values of ~4 GPa, ~3 GPa and ~2 GPa were obtained respectively, for M0.8V, M0.9V and M1.1V.



291

292 Figure 6: Results of EMM-ARM of the three mortars tested, comparison with CC for the reference mortar
 293 and initial setting time by means of penetration resistance test.

294 Table 4: Comparison of EMM-ARM and CC tests for the NHL mortars and corresponding initial setting
 295 times.

Mortar type	Curing days	Elastic modulus from CC (GPa)	Elastic modulus from EMM-ARM (GPa)			Initial setting time (h)		
			M0.8	M0.9	M1.1	M0.8	M0.9	M1.1
S	2	1.5 (-)						
	4	2.8 (0.7)						
	7	3.8 (1.1)				1.50	2.25	14.00
V	2	1.5 (-)	2.2	1.7	1.0			
			2.1	1.8	1.2			
	4	2.4 (0.2)	3.1	2.4	1.5			
			3.1	2.5	1.7			
	7	3.3 (1.3)	4.1	3.3	2.1			
			4.1	3.4	2.4			

296

297 The comparison between the results of elastic modulus obtained by EMM-ARM and by CC for the
 298 reference mortar M0.9V is also shown in Fig. 6 and Table 4 (where the notation S refers to standard
 299 conditions [10] i.e. compacted and unsealed, the notation V refers to vibrated and sealed specimens (see
 300 Section 2.2) and the two values shown for EMM-ARM correspond to each sample). Additionally, results
 301 of CC tests of mortar M0.9S are included. It can be observed that the values obtained from EMM-ARM
 302 are similar to those obtained from CC tests in terms of magnitude and shape of the curve for the reference
 303 mortar vibrated and sealed, M0.9V. Results of both tests in the case of M0.9V differ by only 1.5% at day

304 7 (comparing results from CC with the average of the two samples from EMM-ARM). For the standard
305 mortar, M0.9S, stiffness is higher from day 2, when the specimens were demolded, reaching a difference
306 of 14% at day 7. However, attention is paid to the standard deviation of CC measurements (error bar in
307 Fig. 6 and values in parenthesis in Table 4), it can be observed that they are very high, especially at early
308 ages when they can reach up to 40% (at day 2 only one specimen per mortar type was measured), in
309 comparison to later testing when they normally reach 20% [18, 27]. Therefore, in spite of the fact of
310 M0.9S seeming to be above M0.9V in a systematic manner, this might not be a meaningful difference as
311 both measurements are within the margin of error. A possible reason for this relatively small difference
312 (14% at day 7) can be due to carbonation reaction with CO₂ from the ambient exposure that is allowed to
313 happen in M0.9S as opposed to the sealed condition of M0.9V, which would not allow carbonation.
314 However, previous works [3, 38] have reported that carbonation does not play a significant role until later
315 curing ages (e.g. 14 days onwards) and the main hardening mechanism in the early ages is actually
316 hydration. Further research, therefore, is needed to study the cause of this difference. All things
317 considered, it is therefore inferred that EMM-ARM can be used for very early age testing (e.g. before 2-3
318 days) for assessment of early kinetics. If longer periods of testing are intended, during which carbonation
319 is expected to play a role, then the current set up of EMM-ARM would require adaptations that involve
320 actual demolding of the specimen. This was not an objective of the present research and was thus not
321 pursued further.

322 Moreover, initial setting times of the three mortars are shown in Fig. 6 (vertical dashed lines in the
323 zoom).

324 In view of the available data, a relation between elastic-modulus as obtained by EMM-ARM and the
325 setting time, as obtained by the penetration test was sought. For the reference mortar M0.9V, the initial
326 setting happens at 2.25 hours after casting and the corresponding elastic modulus is 0.10 GPa. For the
327 mortar M0.8V, the initial setting time is at 1.50 hours after casting (Table 4) and at that moment elastic-
328 modulus is around 0.46 GPa measured from the EMM-ARM curve. For mortar M1.1V, the initial setting
329 time is recorded as 14.00 hours and the corresponding elastic modulus is 0.39 GPa. From previous
330 studies, elastic modulus obtained for cement-based materials (pastes) at the moment of setting was found
331 to range between 0.10 and 0.18 GPa [39]. This seems to be coherent with the value obtained for the
332 reference mix M0.9V – 0.10 GPa. However, the values of 0.46 GPa and 0.39 GPa are relatively more

333 dispersed, and the explanation proposed is as follows. The mortar M0.8V appears to have an inherent
334 initial stiffness at time zero, possibly due to the its relatively low water binder ratio, which increases the
335 expected stiffness at the setting time measured. In the case of the mortar M1.1V, it is so fluid (240 mm)
336 that the setting time is delayed quite a bit in addition to which it is also relatively weak. Therefore, in the
337 time interval of 0-14 hours, the mortar had to gain some amount of stiffness before it could offer adequate
338 resistance to penetration. More investigation is needed in order to better understand the range of elastic-
339 moduli that should be expected from NHL mortars at the instant of setting.

340 **3.2 Influence of sample preparation and sealing conditions**

341 In order to be able to relate elastic modulus measurements (through EMM-ARM and CC) of NHL
342 mortars with density, flexural and compressive strength tests, and open porosity, the latter were
343 performed on prismatic specimens prepared and cured according to standard procedures (compacted and
344 unsealed) and according to the ones adopted for EMM-ARM (vibrated and sealed). Also, specimens
345 compacted and sealed were tested to analyze better the influence of each preparation method. The
346 following sub-sections describe the main findings in such concern.

347 **3.2.1 Flexural and compressive strength tests**

348 Flexural and compressive strength were assessed at 2, 4 and 7 days of age on the three mortar mixes
349 with different preparation methods: standard (compacted with 25 strokes of the tamper and unsealed),
350 vibrated and sealed, and compacted and sealed. In Fig. 7, the results of the mixes prepared/cured with
351 standard procedures (M0.8S, M0.9S and M1.1S), are plotted for the flexural strength (a) and the
352 compressive strength (b). Each point represents the mean value of three specimens tested for the flexural
353 strength and the one of the six resulting halves in the case of the compression strength. The error bars are
354 the corresponding standard deviations. The results follow the expected path: mortars with lower
355 water/lime ratios present higher flexural and compressive strengths. The flexural strengths of M0.8S and
356 M0.9S are very similar to each other, in coherence with previous observations for the same mixes that
357 had been studied at the age of 56 days [18].

358 Furthermore, the variability of results between mortars of different batches was tested for compression
359 strength of the reference mortar, M0.9S: it was found to be less than 5% at day 7, implying that the results
360 present good repeatability. Standard deviations of results, as shown in Fig. 7, are also within acceptable

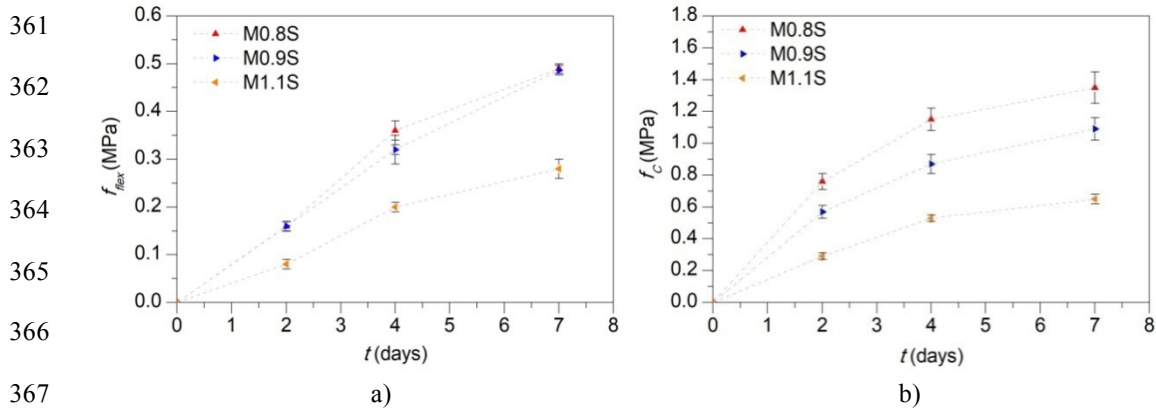


Figure 7: Evolution of: a) flexural, b) compressive strengths with time.

ranges.

In addition, Table 5 shows a comparison between results of different preparation methods (values in brackets refer to the standard deviation). Here, $(f_s - f_v)/f_s$ (%) and $(f_s - f_c)/f_s$ (%) refer to the relative difference of the strength of vibrated and sealed (V) and compacted and sealed (C) specimens, respectively, in relation to the corresponding standard (S) beams. In general, mortars that are sealed provide lower flexural and compressive strengths compared to the standard ones. For example, for the reference mortar, M0.9 (at day 7), the flexural strength is 49% smaller for both mortars that are vibrated and sealed (V) and compacted and sealed (C), as compared to the standard situation (S). Furthermore, in comparison to the standard situation (S), the compressive strength is approximately 21% smaller in the mortars that are vibrated and sealed (V) and 29% in the ones that are compacted and sealed (C). This could be, at least partially, due to the fact that the sealed specimens (kept in the climatic chamber inside

Table 5: Influence of the compacting method and curing conditions on the mechanical properties and comparison with the corresponding standard mortars at day 7.

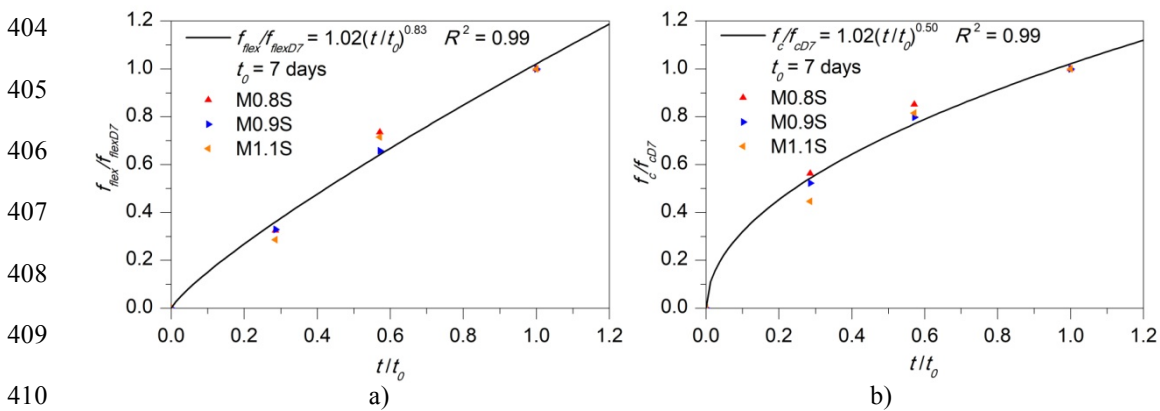
	Flexural strength (MPa)			Compressive strength (MPa)		
	M0.8	M0.9	M1.1	M0.8	M0.9	M1.1
S	0.49 (0.01)	0.49 (0.01)	0.28 (0.02)	1.35 (0.10)	1.09 (0.07)	0.65 (0.03)
V	0.28 (0.06)	0.25 (0.01)	0.14 (0.01)	1.06 (0.04)	0.86 (0.03)	0.47 (0.01)
C	0.28 (0.01)	0.25 (0.02)	0.14 (0.01)	1.07 (0.06)	0.77 (0.06)	0.48 (0.02)
	Decrease on flexural strength (%)			Decrease on compressive strength (%)		
	M0.8	M0.9	M1.1	M0.8	M0.9	M1.1
$\frac{f_s - f_v}{f_s}$ (%)	43	49	50	22	21	27
$\frac{f_s - f_c}{f_s}$ (%)	44	49	49	21	29	26

Note: values in brackets are standard deviations.

383 two plastic bags) were still wet during testing as they could not be air dried in the climatic chamber as the
 384 unsealed ones (just kept in the climatic chamber in contact with the air). A similar phenomenon was
 385 observed in [40], where brick masonry prisms and its components (bricks and three types of cement
 386 mortars with different cement to sand ratios) were air cured at 30°C and RH 90% for 28 days. After this
 387 period, the specimens were divided into three groups and stored in oven-dry state (oven drying at 105°C),
 388 air dry (at 30°C and RH 90%) and wet state (water immersion) for 24 hours. Then, they were tested for
 389 compressive strength, bond test and direct shear test. The results showed that the compressive strength of
 390 the weakest cement mortar could be 15.9% less for wet specimens in comparison to the air dried
 391 specimens (at 30°C and RH 90%). Popovics [41] related this variation between wet and air cured
 392 specimens to the increase of the internal pressure in wet conditions due to a higher amount of water
 393 present in pores. Under this situation, the chance of cracking in a mortar with lesser external load
 394 increases and therefore the compressive strength is reduced. More detailed information on this
 395 phenomenon can be seen in [40].

396 Finally, it is worth remarking that the results of mortars that are vibrated and sealed and compacted
 397 and sealed are quite similar, meaning that the compaction method may not have much influence on the
 398 mechanical strength of NHL mortars at early stages.

399 In addition, the results of flexural and compressive strength of the mortars with the three different
 400 preparation methods were normalized with respect to their values at day 7 (f_{flex}/f_{flexD7} and f_c/f_{cD7} ,
 401 respectively). Then, non-dimensional evolution curves of flexural (Fig. 8 (a)) and compressive (Fig. 8 (b))
 402 strengths with time were obtained as shown for the standard (S) mortar, as the kinetics of evolution was
 403 rather similar in all cases. Equations 6 and 7 and Table 6 show the corresponding non-dimensional



411 Figure 8: Non-dimensional evolution curves of a) flexural and b) compressive strengths with time for the
 412 standard (S) mortar.

413 $\frac{f_{flex}}{f_{flex_{D7}}} = p \left(\frac{t}{t_0}\right)^q$ (6)

414 $\frac{f_c}{f_{c_{D7}}} = r \left(\frac{t}{t_0}\right)^u$ (7)

415

416 Where t_0 are 7 days.

417

Table 6: Coefficients of equations 6 and 7.

		S	V	C	Mean (CoV)
Flexural strength	p	1.02	1.01	1.00	1.01 (1%)
	q	0.83	0.71	0.80	0.78 (8%)
Compressive strength	r	1.02	1.02	1.00	1.01 (1%)
	u	0.50	0.54	0.52	0.52 (4%)

418

419 tendencies for the three mortars with the three preparation methods (standards, S; vibrated and sealed, V;
420 and compacted and sealed, C). These equations can be useful to obtain the flexural and compressive
421 strengths of different NHL mortars at early ages just by knowing their corresponding values at day 7,
422 which can also be useful for numerical models with NHL mortars at early ages.

423 To assess the impact of the three different variables used, namely - preparation method (S, V or C),
424 the time of testing (2, 4 or 7 curing days) and the water/lime ratio (0.8, 0.9 or 1.1), a three-way ANOVA
425 test was performed, using the software Matlab R2016 [42]. In Table 7, p values lower than 0.05 indicate
426 significance of the corresponding factor. Observing the results, it may be concluded that both the
427 preparation method as well as the water/lime ratio do not have a significant effect on the non-dimensional

428 Table 7: Results of a three-way ANOVA of the influence of three factors on the non-dimensional flexural
429 and compressive strengths.

Factors		Analysis on non-dimensional flexural strength	Analysis on non-dimensional compressive strength
		p value	p value
Preparation method (S, V and C)	g_1	0.13	0.24
Testing moment (2, 4 and 7 days)	g_2	0.00	0.00
Water/lime ratio (0.8, 0.9 and 1.1)	g_3	0.70	0.27
Interactions	$g_1 \times g_2$	0.09	0.20
	$g_1 \times g_3$	0.52	0.29
	$g_2 \times g_3$	0.92	0.21

430

431 evolution curves of flexural and compressive strength (p value > 0.05), while, the time of testing does
432 have an influence (p value < 0.05). In addition, from Table 7, it may also be observed that the interaction
433 of the three factors does not have any statistical significance.

434 We have proposed the use of a single value for each of the coefficients p , q , r and u . This is because
435 the percentages of variation from the mean values were found to be low. Furthermore, from the results of
436 ANOVA, it was found that the method of sample preparation did not have a statistically significant
437 impact on the non-dimensional evolution of compressive and flexural. This implies that the two general
438 equations with mean coefficients could be used to describe the non-dimensional evolution of flexural and
439 compressive strengths up to 7 days of curing age, independent of the preparation method and the
440 water/lime ratio.

441 3.2.2 UPV

442 Before performing flexural and compressive strengths, discrete measurements of UPV were taken in
443 the transverse direction of samples at day 2, 4 and 7. In this case, standard mortars (M0.8S, M0.9S and
444 M1.1S) were compared with mortars that are vibrated and sealed (M0.8V, M0.9V and M1.1V) (see Table
445 8, where the values in brackets indicate the standard deviation). Results from Table 4 show a similar trend
446 as the one observed for mechanical properties: mortars with lower water/lime ratios present higher
447 velocities than the ones with higher water/lime ratios. For example, pulse velocity measured on average
448 was 1750 m/s, 1530 m/s and 1300 m/s for M0.8S, M0.9S and M1.1S, respectively, at day 7. Variability of
449 results among mortars of different batches was also checked for the reference mortar, M0.9S, and found
450 to be less than 5% at day 7, confirming good repeatability of the tests. On the other hand, comparison of
451 results between vibrated and sealed counterparts of the standard mortar shows that the latter presents
452 higher values of transverse velocity compared to the standard ones. For example, it was 2070 m/s in the
453 reference mortar vibrated and sealed, M0.9V, while for the standard reference mortar, M0.9S, it was
454 1530 m/s. It is noted that this trend is opposite to the one described for compressive/flexural strength (and
455 even elastic-modulus) described in the previous sections, where the “S” mixes were systematically
456 presenting higher values for mechanical properties compared to “V” mixes. This fact can be interpreted
457 by the influence of water present in the porous network of the specimens during testing, which can play a
458 role in the measured UPV. According to Lencis *et al.* [43] and Lafhaj *et al.* [44], UPV measurements
459 increase with the material’s degree of saturation. For example, for concrete, UPV can be 19% higher in

460 Table 8: Results of UPV in the lateral and longitudinal directions for the standard (S) and vibrated and
 461 sealed (V) mortars.

		Transverse wave velocity (m/s)		
Curing days		M0.8	M0.9	M1.1
S	2	1430 (40)	1230 (80)	-
	4	1530 (20)	1300 (20)	1030 (40)
	7	1750 (50)	1530 (10)	1300 (20)
V	2	1790 (20)	1800 (30)	1500 (60)
	4	1970 (60)	2020 (60)	1550 (200)
	7	2110 (50)	2070 (20)	1630 (80)

462 Note: values in brackets are standard deviations.

463
 464 fully saturated specimens in comparison to the completely dry ones [43]. Also Bungey [45] showed that
 465 UPV in wet concrete specimens was higher than in the corresponding dry ones. Considering this, it is
 466 reasonable that UPV values may be higher in the sealed specimens as they were still wet in the moment
 467 of testing, in comparison to the standard ones that were air dried in the climatic chamber.

468 3.2.3 Density and open porosity

469 Relationships were also established among the physical properties measured on the NHL mortars,
 470 such as wave propagation velocity from UPV, density and open porosity. Density was measured for all
 471 mortars at day 2, 4 and 7 just before performing flexural and compressive strengths (the weight of each
 472 sample was divided by their corresponding volume). In general, the results of density follow the same
 473 trend as that of mechanical properties and UPV (see Table 9 where the values in brackets are the standard
 474 deviation): mortars with lower water/lime ratios present higher values of density. For example, it is
 475 2.08 g/cm³, 2.03 g/cm³ and 1.94 g/cm³, respectively for standard mortars M0.8S, M0.9S and M1.1S. On
 476 the other hand, for all mortar compositions, density tends to decrease with time in the first seven curing
 477 days, probably, due to the evaporation of water present inside the mortars. For instance, it is 2.21 g/cm³ at
 478 day 2 and 2.03 g/cm³ at day 7 for reference mortar M0.9S. Furthermore, comparing mortars that are
 479 sealed with the standard ones, it is observed that the former have higher values of density as their water
 480 content is higher due to the sealed conditions. For example it changed from 2.24 g/cm³ to 2.03 g/cm³
 481 when comparing M0.9V with M0.9S.

482 As for open porosity, standard mortars were compared with the vibrated and sealed ones at day 7, see
 483 Table 10 (again values in brackets are standard deviation). In general, as water/lime ratio increases,

484 Table 9: Results of bulk density at different curing days for the standard (S), vibrated and sealed (V)
 485 and compacted and sealed (C) mortars.

	Curing days	M0.8 (g/cm ³)	M0.9 (g/cm ³)	M1.1 (g/cm ³)
S	2	2.25 (0.01)	2.21 (0.01)	2.17 (0.01)
	4	2.18 (0.02)	2.12 (0.01)	2.06 (0.01)
	7	2.09 (0.01)	2.03 (0.01)	1.94 (0.01)
V	2	2.25 (0.01)	2.25(0.01)	2.20 (0.04)
	4	2.24 (0.01)	2.25 (0.01)	2.18 (0.02)
	7	2.23 (0.01)	2.24 (0.01)	2.17 (0.04)
C	2	2.31 (0.01)	2.28 (0.01)	2.20 (0.01)
	4	2.29 (0.01)	2.28 (0.001)	2.20 (0.01)
	7	2.27 (0.01)	2.27 (0.001)	2.20 (0.01)

486 Note: values in brackets are standard deviations.

487

488 porosity also does, measuring 26.1%, 27.2% and 29.9%, respectively for mortars M0.8S, M0.9S and
 489 M1.1S. Comparing both preparation methods, it was checked that open porosity was slightly higher for
 490 the mortars that are vibrated and sealed in comparison with the standard ones, but in fact this difference is
 491 very low and in most cases it is within the margin of error.

492

493 Table 10: Results of open porosity at day 7 for the standard (S) and vibrated and sealed (V) mortars.

	Curing days	M0.8 (%)	M0.9 (%)	M1.1 (%)
S	7	26.1 (0.3)	27.2 (0.2)	29.9 (0.4)
V	7	26.5 (0.2)	28.0 (0.3)	30.9 (0.2)

494 Note: values in brackets are standard deviations.

495

496 Figure 9 shows some of these tendencies in relation to results of UPV for the standard mortars
 497 (M0.8S, M0.9S and M1.1S) at day 7. In general, it can be observed that as open porosity increases,
 498 density and lateral velocity of UPV decrease. It is logical that density decreases as the number of pores
 499 increases and therefore open porosity also increases with a consequent decrease of the wave propagation

500

501

502

503

504

505

506

507

508

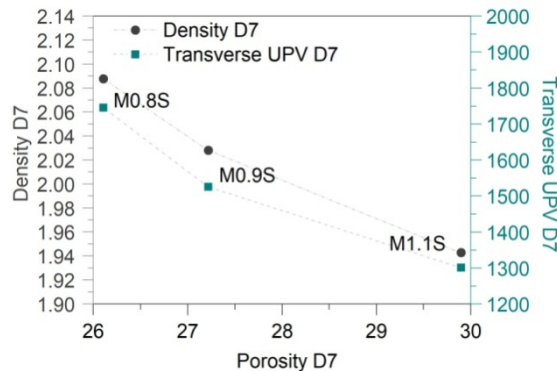


Figure 9: Relationship between open porosity, density and UPV at day 7 for M0.9S.

509 velocity. Similar trends of pulse velocity decreasing with porosity, were also observed by Lafhaj *et al.*
510 [44] for cement mortars.

511 3.3 Thermogravimetric analyses

512 The material was also characterized by means of free portlandite content through thermogravimetric
513 analysis (TGA). For this purpose, tests were performed at day 0, 2, 4 and 7 on the corresponding lime
514 paste, P0.9, of the reference mortar. The samples were sealed until the moment of testing in order to study
515 the evolution of hydration by measurement of free portlandite content and to avoid carbonation reaction.
516 Figure 10 shows the relation between free portlandite content of P0.9 and the compressive strength of
517 mortar M0.9V at the same curing age. It can be observed that portlandite content increases as a function
518 of the compressive strength. A similar trend was also observed by Boualleg *et al.*[46] for cement pastes
519 and mortars. They obtained a linear fitting for different cement samples while we obtain a similar linear
520 adjustment for the same sample at different curing days. Lanas *et al.*[3] also studied the evolution of free
521 portlandite content on NHL mortars and they observed that it increased up to 28 or 91 days depending on
522 the lime/aggregate ratio. In Fig. 10, it may be remarked that the presence of free portlandite at day 0, is
523 typical of the nature of raw material itself. For example, in the work by Arizzi *et al.* [47], the raw NHL
524 3.5 presented a content of portlandite between 40% and 50%. This amount is coherent with results of
525 XRD of the NHL 3.5 of the present study (Table 1 and Fig. 1), where a range between 40% and 45% of
526 portlandite is obtained.

527

528

529

530

531

532

533

534

535

536

537

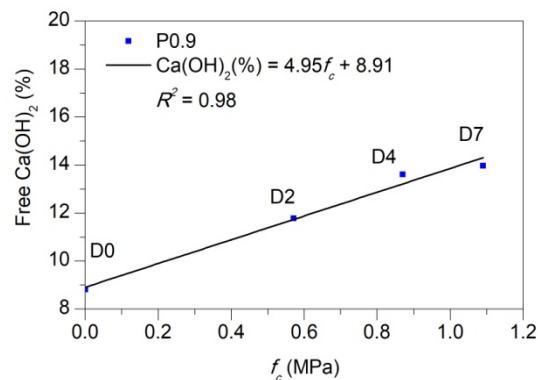


Figure 10: Free portlandite content as a function of compressive strength on the reference sealed paste samples.

538 **4. CONCLUSIONS**

539 In this research, properties of three NHL type 3.5 mortars with different water/lime ratios and same
540 lime/aggregate ratio are studied at early ages, such as density, flexural and compressive strengths,
541 stiffness evolution through EMM-ARM and CC, and the evolution of free portlandite content with time.
542 An exhaustive physical and mechanical characterization was performed on the material under different
543 fabrication and curing methods: standard procedures (compacting and unsealing), vibration and sealing,
544 and compacting and sealing. The results show good repeatability in the tests, especially in EMM-ARM,
545 flexural and compressive strength tests. The following main conclusions can be extracted from this
546 research:

547 (1) The EMM-ARM method has shown feasible potential of application to the study of NHL
548 mortars at early ages (< 3-7 days), with very good repeatability and comparability with results
549 obtained from CC testing (with both standard compaction/curing and non-standard curing
550 involving vibration and sealing). The initial dormant period was well captured, as well as the
551 entire kinetics of stiffness increase, which was clearly different amongst the three studied
552 mortars. As time passes, the standard curing condition allows specimens to harden further, the
553 results attained by EMM-ARM (in sealed conditions) start to deviate from the CC results with
554 standard curing (less stiffness assessed by EMM-ARM). Therefore, if EMM-ARM is to be
555 applied for longer durations, more than a mere couple of days, adaptations to the test setup are
556 necessary, so as to allow carbonation. These adaptations will bring new challenges due to mass
557 variations of the specimen during testing, which will need to be monitored, so as to provide
558 adequate estimates of elastic-modulus (obtained through the dynamic equation of motion that
559 requires the mass of the specimen which is no longer constant).

560 (2) Flexural and compressive strengths behave as expected: mortars with lower water/lime ratios
561 present higher strengths. Comparing standard- i.e., air cured specimens (S) with the ones that are
562 sealed (V and C), it is observed that the latter have lower strength. These results were
563 unexpected since the sealed specimens were subjected to more humid moisture curing conditions
564 and therefore higher degrees of hydration. One possible explanation for this may be that the
565 sealed specimens were more wet at the moment of testing compared to the unsealed specimens
566 (subjected to air curing) and therefore exhibited lower values of mechanical strength as

567 discussed by other researchers [40, 41]. Further research would be needed to study the effect of
568 wetting conditions on NHL mortars.

569 (3) Furthermore, the evolution tendencies of normalized flexural and compressive strength with
570 respect to their corresponding values at day 7 were obtained. These formulas could be useful for
571 numerical models with NHL mortars at early ages. It must be noted though, that these evolution
572 trends have been presented specifically with regard to mixes having lime/aggregate ratio of 1:3
573 (by volume) and employing limestone aggregates.

574 (4) Discrete measurements of UPV were also taken in the transverse direction of the prismatic
575 specimens just before performing flexural and compressive strength tests. The results showed
576 that pulse velocity increased with lower water/lime ratios. Furthermore, velocity also increased
577 in specimens that were more humid, such as the sealed ones. This is possibly related to
578 longitudinal waves propagating faster through pores filled with water than through the ones
579 filled with air [48]. Such tendencies appear to be similar to the ones found by Lencis *et al.* [43],
580 Lafhaj *et al.* [44] and Bungey [45]. This caused the sealed specimens to exhibit higher UPV than
581 the standard cured specimens, which is an opposing trend to the one found in other mechanical
582 tested properties (strength and stiffness). A word of caution is thereby issued on potentially
583 misleading observations that might be taken when comparing UPV test results of specimens
584 cured under different conditions.

585 (5) Density follows the same trend as flexural and compressive strength and UPV: it is higher for
586 mortars with lower water/lime ratios. Comparing specimens that are sealed with the standard
587 ones, it was observed that the former has higher values of density as they are more humid.

588 (6) Open porosity was measured at day 7 and, as expected it increases with higher water/lime ratios.
589 In general, it was observed that density and pulse velocity decreased as open porosity increased.

590 (7) Finally, the evolution of free portlandite content was measured in the reference lime paste at
591 days 0, 2, 4 and 7. It was related to the compressive strength of the mortar with the same
592 composition at corresponding ages. This relation was adjusted with a linear fitting up to day 7.
593 Other authors [3] also observed that free portlandite content increased up to day 28 or 91
594 depending on the lime/aggregate ratio of NHL mortars.

595 ACKNOWLEDGEMENTS

596 The authors wish to thank the funding provided by the Portuguese Foundation for Science and
597 Technology (FCT) to the Research Projects and PTDC/ECM-EST/1056/2014 (POCI-01-0145-FEDER-
598 016841), as well to the Research Unit ISISE (POCI-01-0145-FEDER-007633), also from the *Ministerio*
599 *de Economía y Competitividad*, Spain, under grant BIA2015-68678-C2-1-R. Lucía Garijo acknowledges
600 financial support from the scholarship FPU014/05186 awarded by the *Ministerio de Educación, Cultura y*
601 *Deporte*, Spain, from the scholarship 2016/11635 given by *Universidad de Castilla-La Mancha* (UCLM)
602 to do a research stay in another institution and from the research project RTC-2017-6736-3 awarded by
603 the *Ministerio de Ciencia, Innovación y Universidades*, Spain. Advice on the fabrication of NHL mortars
604 provided by Prof. Pere Roca from *Universidad Politécnica de Cataluña* are also much appreciated. We
605 also thank the research group of Prof. Anselmo Acosta in UCLM for their help on the chemical and
606 mineralogical analyses of the raw NHL and the company *Iesmat, Instrumentación específica de*
607 *materiales*, for the laser particle size distribution of the raw NHL.

608 REFERENCES

- 609 [1] Kalagri A, Karatasios I, Kilikoglou V. The effect of aggregate size and type of binder on
610 microstructure and mechanical properties of NHL mortars. *Construction and Building Materials*.
611 2014;53:467-74.
- 612 [2] Chan R, Bindiganavile V. Toughness of fibre reinforced hydraulic lime mortar. Part-1: Quasi-static
613 response. *Materials and Structures*. 2010;43(10):1435-44.
- 614 [3] Lanás J, Bernal JLP, Bello MA, Galindo JIA. Mechanical properties of natural hydraulic lime-based
615 mortars. *Cement and Concrete Research*. 2004;34(12):2191-201.
- 616 [4] Arandigoyen M, Alvarez JI. Pore structure and mechanical properties of cement-lime mortars. *Cement*
617 *and Concrete Research*. 2007;37(5):767-75.
- 618 [5] Azenha M, Magalhaes F, Faria R, Cunha A. Measurement of concrete E-modulus evolution since
619 casting: A novel method based on ambient vibration. *Cement and Concrete Research*. 2010;40(7):1096-
620 105.
- 621 [6] Azenha M, Ramos LF, Aguilar R, Granja JL. Continuous monitoring of concrete E-modulus since
622 casting based on modal identification: A case study for in situ application. *Cement & Concrete*
623 *Composites*. 2012;34(7):881-90.
- 624 [7] Azenha M, Faria R, Magalhaes F, Ramos L, Cunha A. Measurement of the E-modulus of cement
625 pastes and mortars since casting, using a vibration based technique. *Materials and Structures*. 2012;45(1-
626 2):81-92.
- 627 [8] Azenha M. Numerical Simulation of The Structural Behaviour of Concrete Since its Early Ages. [PhD
628 Thesis]: Faculty of Engineering of the University of Porto; 2009.
- 629 [9] Azenha M, Magalhães F, Ramos L. Method based in ambient vibrations for quantifying the evolution
630 of E-modulus of hardening materials. Portugal patent application 104413. 2009.
- 631 [10] BS EN 1015-11. Methods of test for mortar for masonry – Part 11: Determination of flexural and
632 compressive strength of hardened mortar: BSI; 1999/A1:2006. p. 12.
- 633 [11] BS EN 459-1. Building lime – Part 1: Definitions, specifications and conformity criteria. Brussels,
634 Belgium: BSI; 2015. p. 52.
- 635 [12] BS EN 1015-1. Methods of test for mortar for masonry – Part 1: Determination of particle size
636 distribution (by sieve analysis): BSI; 1998/A1:2006. p. 8.

- 637 [13] BS EN 1097-6. Test for mechanical and physical properties of aggregates – Part 6: Determination of
638 particle density and water absorption: BSI; 2013. p. 54.
- 639 [14] BS EN 1097-3. Test for mechanical and physical properties of aggregates – Part 3: Determination of
640 loose bulk density and voids: BSI; 1998. p. 10.
- 641 [15] BS EN 1015-3. Methods of test for mortar for masonry – Part 3: Determination of consistence of
642 fresh mortar (by flow table): BSI; 1999/A2:2006. p. 10.
- 643 [16] BS EN 1015-6. Methods of test for mortar for masonry – Part 6: Determination of bulk density of
644 fresh mortar: BSI; 1998/A1:2006. p. 8.
- 645 [17] BS EN 1015-2. Methods of test for mortar for masonry – Part 2: Bulk sampling of mortars and
646 preparation of test mortars: BSI; 1998/A1:2006. p. 8.
- 647 [18] Garijo L, Zhang XX, Ruiz G, Ortega JJ, Wu Z. The effects of dosage and production process on the
648 mechanical and physical properties of natural hydraulic lime mortars. *Construction and Building
649 Materials* 2018;169:325-34.
- 650 [19] Grilo J, Silva AS, Faria P, Gameiro A, Veiga R, Velosa A. Mechanical and mineralogical properties
651 of natural hydraulic lime-metakaolin mortars in different curing conditions. *Construction and Building
652 Materials*. 2014;51:287-94.
- 653 [20] Lanás J, Sirera R, Alvarez JI. Study of the mechanical behavior of masonry repair lime-based
654 mortars cured and exposed under different conditions. *Cement and Concrete Research*. 2006;36(5):961-
655 70.
- 656 [21] Maia L, Azenha M, Faria R, Figueiras J. Influence of the cementitious paste composition on the E-
657 modulus and heat of hydration evolutions. *Cement and Concrete Research*. 2011;41(8):799-807.
- 658 [22] Maia L, Azenha M, Geiker M, Figueiras J. E-modulus evolution and its relation to solids formation
659 of pastes from commercial cements. *Cement and Concrete Research*. 2012;42(7):928-36.
- 660 [23] Granja JL, Azenha M, de Sousa C, Ferreira C. Comparison Between Different Experimental
661 Techniques for Stiffness Monitoring of Cement Pastes. *Journal of Advanced Concrete Technology*.
662 2014;12(2):46-61.
- 663 [24] Granja J, Azenha M. Towards a robust and versatile method for monitoring E-modulus of concrete
664 since casting: Enhancements and extensions of EMM-ARM. *Strain*. 2017;53(4).
- 665 [25] Ramesh M, Azenha M, Lourenço PB. Mechanical properties of lime-cement masonry mortars in
666 their early ages. *Materials and Structures*. 2019;52(1).
- 667 [26] Granja J, Azenha M. Elastic Modulus Measurement through Ambient Response Method. User's
668 Guide. University of Minho.
- 669 [27] Garijo L, Zhang XX, Ruiz G, Ortega JJ, Yu RC. Advanced mechanical characterization of NHL
670 mortars and cohesive simulation of their failure behavior. *Construction and Building Materials*.
671 2017;153:569-77.
- 672 [28] ASTM. C403/C 403M-99. Standard Test Method for Time of Setting of Concrete Mixtures by
673 Penetration Resistance. West Conshohocken, United States: ASTM; 1999.
- 674 [29] Meyers MA, Chawla KK. *Mechanical Behavior of Materials*. Second Edition. New York, USA:
675 Cambridge University Press; 2008.
- 676 [30] UNE 83980. Concrete durability – Test methods – Determination of the water absorption, density
677 and accessible porosity for water in concrete. Madrid: AENOR; 2014. p. 8.
- 678 [31] Montoya C, Lanás J, Arandigoyen M, Navarro I, Casado PJG, Alvarez JI. Study of ancient dolomitic
679 mortars of the church of Santa Maria de Zamarce in Navarra (Spain): comparison with simulated
680 standards. *Thermochimica Acta*. 2003;398(1-2):107-22.
- 681 [32] Parrott LJ, Killoh DC. Carbonation in a 36 year old, in-situ concrete. *Cement and Concrete
682 Research*. 1989;19(4):649-56.
- 683 [33] Oliveira MA, Azenha M, Lourenço PB, Meneghini A, Guimaraes ET, Castro F, Soares D.
684 Experimental analysis of the carbonation and humidity diffusion processes in aerial time mortar.
685 *Construction and Building Materials*. 2017;148:38-48.
- 686 [34] Silva DA, Wenk HR, Monteiro PJM. Comparative investigation of mortars from Roman Colosseum
687 and cistern. *Thermochimica Acta*. 2005;438(1-2):35-40.
- 688 [35] Scrivener K, Snellings R, Lothenbach B. A practical Guide to Microstructural Analysis of
689 Cementitious Materials. In: Press C, editor.: Taylor & Francis Group; 2016.
- 690 [36] Oliveira MA. A Multi-Physics Approach Applied to Masonry Structures with Non-Hydraulic Lime
691 Mortars [PhD Thesis]. Guimaraes, Portugal: University of Minho; 2015.
- 692 [37] Lawrence RMH, Mays TJ, Walker P, D'Ayala D. Determination of carbonation profiles in non-
693 hydraulic lime mortars using thermogravimetric analysis. *Thermochimica Acta*. 2006;444(2):179-89.

- 694 [38] Cizer O. Competition between carbonation and hydration on the hardening of calcium hydroxide and
695 calcium silicate binders. [PhD Thesis]: Haverlee (Belgium): Katholieke Universiteit Leuven 2009.
- 696 [39] Granja JL. Continuous characterization of stiffness of cement-based materials: experimental analysis
697 and micro-mechanics modelling. [PhD Thesis]: Universidade do Minho, Escola de Engenharia; 2016.
- 698 [40] Sathiparan N, Rumeskumar U. Effect of moisture condition on mechanical behavior of low strength
699 brick masonry. *Journal of Building Engineering*. 2018;17:23-31.
- 700 [41] Popovics S. *Strength and Related Properties of Concrete: A Quantitative Approach*. Wiley, New
701 York 1998.
- 702 [42] MathWorks, Moler C. *Matlab*. R2016b ed2016.
- 703 [43] Lencis U, Udris A, Korjakins A. Moisture Effect on the Ultrasonic Pulse Velocity in Concrete Cured
704 under Normal Conditions and at Elevated Temperature. *Construction Science* 2013/14:71-8.
- 705 [44] Lafhaj Z, Goueygou M, Djerbi A, Kaczmarek M. Correlation between porosity, permeability and
706 ultrasonic parameters of mortar with variable water/cement ratio and water content. *Cement and Concrete*
707 *Research*. 2006;36(4):625-33.
- 708 [45] Bungey JH. The validity of Ultrasonic Pulse Velocity testing of in-place concrete for strength. *Ndt*
709 *International*. 1980;13(6):296-300.
- 710 [46] Boualleg S, Bencheikh M, Belagraa L, Daoudi A, Chikouche MA. The Combined Effect of the
711 Initial Cure and the Type of Cement on the Natural Carbonation, the Portlandite Content, and
712 Nonevaporable Water in Blended Cement. *Advances in Materials Science and Engineering*. 2017:1-17.
- 713 [47] Arizzi A, Cultrone G, Brummer M, Viles H. A chemical, morphological and mineralogical study on
714 the interaction between hemp hurds and aerial and natural hydraulic lime particles: Implications for
715 mortar manufacturing. *Construction and Building Materials*. 2015;75:375-84.
- 716 [48] Albert DG. A comparison between wave propagation in water-saturated and air-saturated porous
717 materials. *Journal of Applied Physics*. 1993;73(28):28-36.